



Trends in
**Applied Sciences
Research**

ISSN 1819-3579



Academic
Journals Inc.

www.academicjournals.com

Effect of Vertical Contraction Joints on Thermo-Static Stability of Karun-1 Arch Dam

M. Labibzadeh and A. Khajehdezfuly

Department of Civil Engineering, Faculty of Engineering, Shahid Chamran University, Ahvaz, Iran

Corresponding Author: M. Labibzadeh, Department of Civil Engineering, Faculty of Engineering, Shahid Chamran University, Ahvaz, Iran

ABSTRACT

In this study, effect of vertical contraction joints on the Karun-1 arch concrete dam safety certainly under effect of thermal loads was looked over by means of the relatively 3D finite elements exact simulation of the geometric, material behavior and boundary conditions of the dam using ABAQUS package. This software has good potentials for modeling three dimensional heat transfer thorough dam volume. Arch, cantilever and principal stress tensors as well as displacement vectors were selected as stability indexes safety control and deeply examined. It was revealed that the contraction joints have significant effects in the thermo-static response of the dam and if any of two important factors e.g., contraction joints or thermal effects are not considered in Kurun-1 dam processing, the significant errors in computing displacements and stresses and consequently in dam stability qualification can be occurred.

Key words: Heat transfer, thermal effects, vertical blocks, upstream, downstream, ABAQUS

INTRODUCTION

Arch dams are huge complicated facilities built mainly for water and electric power supply usually in dry and semi-dry climate countries such as Iran. Karun-1 dam is an aged high elevated concrete arch dam located in north western of Khouzestan province of Iran country near the Masjed-Soleiman city which its building was completed in 1962. Under the effect of operation and climate conditions as well as dam body internal chemical reactions such as cement hydration and alkali-silica reaction, Karun-1 aged high elevated concrete arch dam experiences some of changes in its structural characteristics like concrete modulus of elasticity of dam body. In recent years, safety control of this dam is highlighted due to the fact that the electrical energy generation of the dam has been increased thorough the development of the second phase of its power plant. In order to prevention of initiation and growth of thermal cracks in dam body, it has been normal procedure to provide vertical contraction joints in arch dams at approximately 15 to 20 m spacing. In this way, continuous dam body is separated to several vertical blocks mainly named monoliths in scientific literatures. These contraction joints were injected with cement grout after the concrete has cooled to mean temperature. It is worth to mention that adjacent blocks has no any relative shear motions and even under strong ground shakings some little dislocations were reported and many studies conducted till now were focused on the investigation about the effects of contraction joints on earthquake response of the arch dams (Fenves *et al.*, 1992; Zhang *et al.*, 2000; Xinja *et al.*, 2002; Arabshahi and Lotfi, 2009; Jing and Chen, 2009; Sheng *et al.*, 2009; Li *et al.*, 2008; Zhao *et al.*,

2007; Du and Tu, 2007). However, an arch dam in compare to gravity dam has a wider surface and less thickness, so, temperature differences between upstream and downstream faces of these dams can lead to creation of larger stress and strains in relative to their corresponding values in gravity dams. In a few works has been performed to date on thermal analysis of arch dams, one dimensional heat transfer across the vertical section of dam has been studied in which the influence of vertical contraction joints were not included (Sheibani and Ghaemian, 2006). They incorporated the thermal stress field in Karaj arch dam in Iran. They contributed in their study the effect of solar radiations as well as other resources of heat generation in dam like air and reservoir temperature changes. They concluded that two dimensional thermal analysis of an arch dam cannot yield accurate results and 3D numerical simulation is needed. Ardito *et al.* (2008) investigated the effect of seasonal thermal loading as well as hydrostatic pressure on an arch dam in Italy. They used truncated Fourier series for heat transfer calculation across dam thickness. They computed damage diagnosis thorough minimization of a batch discrepancy function between measured and computed displacements as inverse analysis in a linear thermo-elasticity context. Léger and Leclerc (2007) presented frequency domain solution algorithms of one dimensional transient heat transfer equation to accommodate thermal analysis of Schlegeis arch dam. They developed two algorithms to solve two kinds of heat transfer problems: direct problems in which temperature variations are specified on both upstream and downstream faces of dam and inverse problems where temperatures are measured with thermometers located inside instrumented dam sections. Léger and Seydou (2009) presented the hybrid dam displacement model to simulate the seasonal thermal displacements of gravity concrete dams. They used their model for predict the behavior of dam under extreme thermal effects which cannot be happened in real conditions.

According to what mentioned above, in this research a try has been done to study the effect of vertical contraction joints on the Karun-1 dam safety certainly under effect of thermal loads by means of a relatively 3D exact simulation of the geometric, material behavior and boundary conditions of the dam using ABAQUS finite elements package. ABAQUS is commercial powerful software for finite elements analysis developed by HKS Inc of Rhode Island, USA and marketed under the SIMULIA brand of Dassault Systemes DS. The ABAQUS product suite consists of three core products: ABAQUS/Standard, ABAQUS/Explicit and ABAQUS/CAE. ABAQUS/Standard is a general-purpose solver using a traditional implicit integration scheme to solve finite element analyses. ABAQUS/Explicit uses an explicit integration scheme to solve highly nonlinear transient dynamic and quasi-static analyses. ABAQUS/CAE provides an integrated modeling (preprocessing) and visualization (post processing) environment for the analysis products. The ABAQUS is used in the automotive, aerospace and industrial product industries. The product is popular with academic and research institutions due to the wide material modeling capability and the program's ability to be customized. Principal stress tensors, displacement vectors and strain energy were selected as stability indexes safety control and examined. It will be shown that the contraction joints have significant effects on the thermo-static behavior of Karun-1 dam.

MATERIALS AND METHODS

As it has been emphasized, in this study we are going to investigate the effect of vertical contraction joints embedded in a typical arch dam on its thermo-mechanical behavior. To accommodate this issue, thorough May to November 2009 the contraction joints of Karun-1 dam were modeled using small-sliding contact feature of well-known scientific package ABAQUS. In small-sliding contact theory it is assumed that two contact surfaces has only relatively small sliding

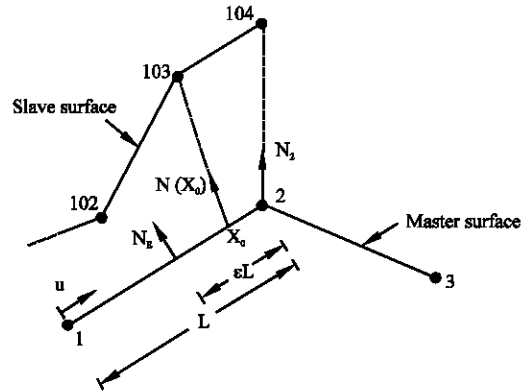


Fig. 1: Slave nodes interacting with a two dimensional surface

relative to each other but arbitrary rotation of the bodies is permitted. In this program two kind of surface is defined: slave surface and master surface through them we can define the contact physical phenomenon. A kinematic constraint that the slave surface node can not penetrate the master surface is enforced. Four internal contact elements designed in the program to handle all kinematic constraint conditions. The three dimensional contact between a slave node and a deformable master surface is selected for the proposed study. For better understanding of relations which will be come into next discussion, the formulation of this kind of contact is presented as below (ABAQUS, Inc. and Dassault Systemes). In this case, a two dimensional slave node interacting with a first order master surface. This formulation can be generalized to second order as well as three dimensional situations.

As shown in Fig. 1, the nodes 102, 103 and 104 are located on slave surface and nodes 1, 2 and 3 are positioned on master surface. In the first step, unit normal vectors are computed for all the nodes on the master surface. For instance, the unit normal N_2 is computed by averaging the unit normal vectors of segments 1-2, 2-3. The user can also define unit normal vector for each node on master surface. Software assigns additional unit normal vectors for each segment a distance ϵL from each end of the segment. N_ϵ is the unit normal vector in the middle of segment 1-2. The unit normals computed are then used to define a smooth varying normal vector, $N(X)$, at any point, X , on the master surface. An 'anchor' point on the master surface X_0 is computed for each slave node so that the vector formed by the slave node and X_0 coincides with the normal vector $N(X_0)$. Assume that the anchor point of slave node 103 is X_0 on the segment 1-2. Then we define:

$$X_0 = X(u_0) = (1 - u_0)X_1 + u_0X_2 \quad (1)$$

where, X_1 and X_2 are the coordinates of nodes 1 and 2, respectively and u_0 is calculated so that $X_0 - X_{103}$ coincides with $N(X_0)$. Furthermore, the contact plane tangent direction, v_0 , at X_0 is selected so that it is perpendicular to $N(X_0)$; i.e.,

$$v_0 = N(X_0) \times e_z = T \cdot \frac{\partial X(u_0)}{\partial u} = T \cdot (X_2 - X_1) \quad (2)$$

where, T is a (constant) rotation matrix.

The small-sliding contact constraint is achieved by requiring that slave node 103 interact with the tangent plane whose current anchor point coordinates are, at any time, given by:

$$\mathbf{x}_0 = N_1(\mathbf{u}_0)\mathbf{x}_1 + N_2(\mathbf{u}_0)\mathbf{x}_2 \quad (3)$$

where, $N_1(\mathbf{u}_0) = 1 - u_0$ and $N_2(\mathbf{u}_0)$ and whose current tangent direction is given by:

$$\mathbf{v} = T.(N_1^u(\mathbf{u}_0)\mathbf{x}_1 + N_2^u(\mathbf{u}_0)\mathbf{x}_2) \quad (4)$$

where, $N_1^u(\mathbf{u}_0) = -1$ and $N_2^u(\mathbf{u}_0)$. Since, the above expressions for the point \mathbf{x}_0 and the vector \mathbf{v} resulted from barycentric (affine) combination of the points \mathbf{x}_1 and \mathbf{x}_0 that is (Christopher, 2007):

$$N_1(\mathbf{u}_0) + N_2(\mathbf{u}_0) = 1 \quad (5a)$$

$$N_1^u(\mathbf{u}_0) + N_2^u(\mathbf{u}_0) = 0 \quad (5b)$$

The contact plane will be mapped properly under affine transformations such as translation, scaling (stretching) and rotation. At each slave node that can come into contact with master surface we construct a measure of over-closure h (penetration of the node into the master surface) and measures of relative slip s_i . These kinematic measures are then used, together with appropriate Lagrange multiplier techniques, to introduce interaction theories as will be described later. In three dimensions, the over-closure h along the unit contact normal \mathbf{n} between a slave point \mathbf{x}_{N+1} and a master plane $p(\zeta_1, \zeta_2)$, where, ζ_i parametrize the plane, is determined by finding the vector $(p - \mathbf{x}_{N+1})$ from the slave node to the plane that is perpendicular to the tangent vector \mathbf{v}_1 and \mathbf{v}_2 at p . Mathematically, we express the required condition as:

$$\mathbf{h}\mathbf{n} = p(\xi_1, \xi_2) - \mathbf{x}_{N+1} \quad (6)$$

When:

$$\begin{aligned} \mathbf{v}_1 \cdot (p(\xi_1, \xi_2) - \mathbf{x}_{N+1}) &= 0; \\ \mathbf{v}_2 \cdot (p(\xi_1, \xi_2) - \mathbf{x}_{N+1}) &= 0 \end{aligned} \quad (7)$$

If at a given slave node $h < 0$, there is no contact between the surfaces at that node and no further surface interaction calculations are needed. If $h \geq 0$, the surfaces are in contact. The contact constraint $h = 0$ is enforced by introducing a Lagrange multiplier, \bar{p} , whose value provides the contact pressure at the point. To enforce the contact constraint, we need the first variation δh and for the Newton iterations, we need the second variation $d\delta h$. Likewise, if frictional forces are to be transmitted across the contacting surfaces, the first variation of relative slip δs_i and the second variations $d\delta s_i$ are needed in the formulation. The three dimensional small-sliding deformable contact formulations presented here (Chen and Hisada, 2007; Puso and Laursen, 2002). A point on the contact plane associated with a slave node \mathbf{x}_{N+1} is represented by the vector:

$$p(\xi_1, \xi_2) = x_0 + \xi_1 v_1 + \xi_2 v_2 \quad (8)$$

where, the plane's anchor point x_0 and its two tangent vectors v_1 and v_2 are functions of the current master node coordinates x_0, \dots, x_N . Linearization of Eq. 6 yields:

$$\delta h n + h \delta n = \delta x_0 + \delta \xi_1 v_1 + \xi_1 \delta v_1 + \delta \xi_2 v_2 + \xi_2 \delta v_2 - \delta u_{N+1} \quad (9)$$

where, $\delta x_0 = f(\delta x_1, \dots, \delta x_N)$ and $\delta v_i = g_i(\delta x_0, \dots, \delta x_N)$.

Taking the dot production of Eq. 9 with n results in the following expression for δh :

$$\delta h = -n \cdot (\delta u_{N+1} - \delta x_0 - \xi_1 \delta v_1 - \xi_2 \delta v_2) \quad (10)$$

Likewise, taking the dot product of Eq. 9 with $t_1 = v_1 / \|v_1\|$ and setting $h = 0$ results in the following expression for the variation of the first slip component:

$$\delta s_1 \stackrel{\text{def}}{=} \delta \xi_1 v_1 \cdot t_1 = t_1 \cdot (\delta u_{N+1} - \delta x_0 - \xi_1 \delta v_1 - \xi_2 \delta v_2) \quad (11)$$

Similarly, taking the dot product of Eq. 9 with $t_2 = v_2 / \|v_2\|$ and setting $h = 0$ results in the following expression for the variation of the second slip component:

$$\delta s_2 \stackrel{\text{def}}{=} \delta \xi_2 v_2 \cdot t_2 = t_2 \cdot (\delta u_{N+1} - \delta x_0 - \xi_1 \delta v_1 - \xi_2 \delta v_2) \quad (12)$$

After formulation of small-sliding contact theory, the next step is the surface interaction description. For modeling the normal and in-plane behavior of monoliths interactions in Karun-1 arch dam body, in this research, the Hard contact and Coulomb contact theory were implemented as constitutive models respectively (Franco and Royer-Carfagni, 2005). In Hard contact hypothesis, we have:

$$\begin{aligned} p &= 0 \quad \text{for } h < 0 \quad (\text{open}) \quad \text{and} \\ h &= 0 \quad \text{for } p > 0 \quad (\text{closed}) \end{aligned} \quad (13)$$

where, p is the contact pressure between two surfaces and h is the over-closure at a given point. The contact constraint is enforced with a Lagrange multiplier representing the contact pressure in a mixed formulation. The virtual work contribution is:

$$\delta \Pi = \delta p h + p \delta h \quad (14)$$

And the linearized form of the contribution is:

$$d\delta \Pi = \delta p dh + dp \delta h \quad (15)$$

And in Coulomb constitutive models below relations are used:

$$\tau_{eq} = \sqrt{\tau_1^2 + \tau_2^2} \quad (16)$$

where, τ_{eq} is the equivalent shear stress at a point on the contact surface and τ_1 and τ_2 are the shear stresses in two orthogonal directions in contact surface at the same point. If the τ_{eq} is less than a critical value τ_{crit} which can be defined based on any constitutive rational computations, no relative motion occurs between two contact surfaces. In this study, the τ_{crit} is defined as:

$$\tau_{crit} = \mu p \quad (17)$$

In which, μ is the friction coefficient that is defined simply as the:

$$\mu = \tan \Phi \quad (18)$$

where, Φ is the internal friction angle between two adjacent monoliths (vertical contraction joints) surfaces. In this research, the μ is set to be equal 10 to guarantee that no any relative shear movements are possible at contraction joints. To complete the behavior definition of interaction between adjacent blocks in our arch dam, we must describe the heat flow across an interface via conduction. It is assumed that heat transfer can occur only in the normal direction. Heat conduction across the vertical contraction joints is supposed as below in the present study (Sheibani and Ghaemian, 2006):

$$q = k(\theta_A - \theta_B) \quad (19)$$

where, q is the heat flux per unit area crossing the joint from point A on one surface to point B on the other, θ_A and θ_B are the temperatures of the points on the surfaces and k is the gap conductance. The derivatives of q are:

$$\begin{aligned} \frac{\partial q}{\partial \theta_A} &= k + \frac{1}{2} \frac{\partial q}{\partial \bar{\theta}} (\theta_A - \theta_B) \\ \frac{\partial q}{\partial \theta_B} &= k + \frac{1}{2} \frac{\partial q}{\partial \bar{\theta}} (\theta_A - \theta_B) \end{aligned} \quad (20)$$

Where:

$$\bar{\theta} = \frac{1}{2} (\theta_A + \theta_B)$$

The contribution to the variational statement of thermal equilibrium is:

$$\delta \Pi = qA\delta\theta_A - qA\delta\theta_B \quad (21)$$

where, A is the area. The contribution to the Jacobian matrix for the Newton solution is:

$$d\delta\Pi = dqA\delta\theta_A - dqA\delta\theta_B \quad (22)$$

Where:

$$dq = \frac{\partial q}{\partial \theta_A} d\theta_A + \frac{\partial q}{\partial \theta_B} d\theta_B \quad (23)$$

In this study, we consider the tied thermal contact. This means that the temperature at point A is constrained to have the same temperature as point B. the Lagrange multiplier method is used to impose the constraint by augmenting the thermal equilibrium statement as follows:

$$\delta\Pi = \delta\lambda(\theta_A - \theta_B) + \lambda(\delta\theta_A - \delta\theta_B) \quad (24)$$

where, λ is the Lagrange multiplier. The contribution to Jacobian matrix for Newton solution is:

$$d\delta\Pi = \delta\lambda(d\theta_A - d\theta_B) + d\lambda(\delta\theta_A - \delta\theta_B) \quad (25)$$

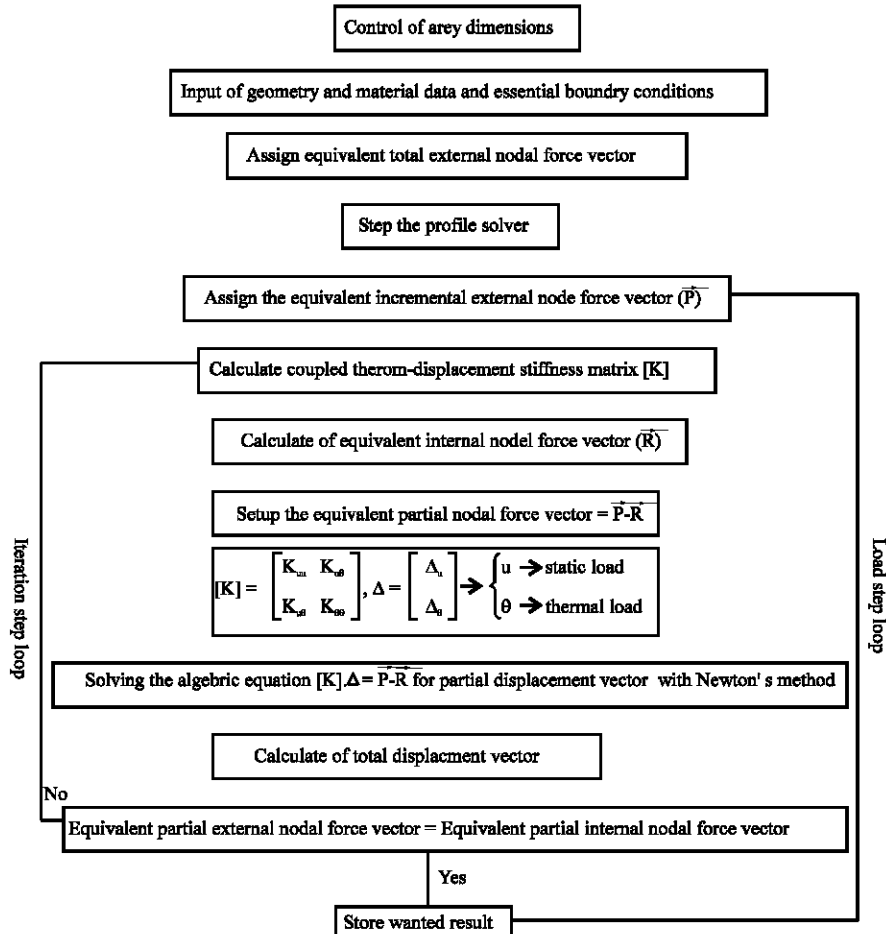


Fig. 2: Numerical solution consequences

At this stage, it is supposed that the theoretical background necessary for doing our proposed problem is approximately prepared. Flowchart of numerical solution based on the mentioned theory is outlined as Fig. 2. Figure 2 shows that solving this problem encounter nonlinear coupled displacement-thermal boundary value analysis. Solution involves an incremental procedure and convergence in each increment obtained only after that equivalent internal nodal force vector is balanced with equivalent external nodal force vector within desirable tolerance.

RESULTS AND DISCUSSION

Four model of Karun-1 arch dam was simulated in order to reach better clarify of the effect of vertical contraction joints in thermo-static dam behavior. Model A considers dam body as a continuous volume without seeing the vertical adjacent block interactions in two loading mode: with (A1) and without (A2) thermal forces. Model B involves the same two loading condition (B1 and B2) with this difference that vertical contraction joints between monoliths have been simulated in the analysis.

In Fig. 3, the 3D finite elements model of dam and its abutments is shown. The types of the elements used in this mesh were selected as C3D20RT for dam body and for abutments as



Fig. 3: Finite elements model of Karun-1 concrete arch dam

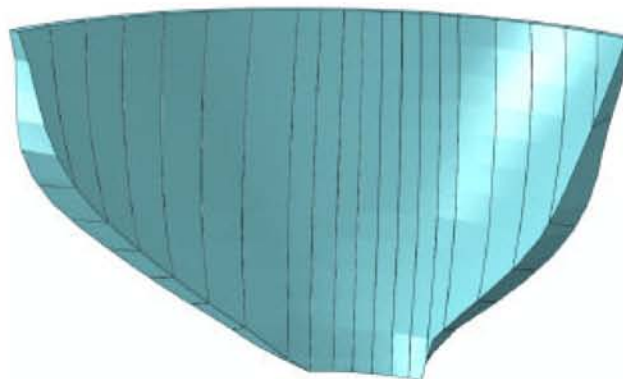


Fig. 4: Vertical contraction joints in Karun-1 dam

C3D10MT. Total number of nodes of the mesh was 110253 and corresponding value for the elements was 47102. Figure 4 indicates the positions of the contraction joints in Karun-1 dam. Upstream-downstream displacements along the highest vertical section of Karun-1 dam which is named usually as central cantilever in arch dam engineering literature have been shown in Fig. 5. The height level of bottom and top of this cantilever are 342 and 542 m from sea level, respectively. Figure 6 shows the trend of movements along central cantilever in gravity direction. Four model results were compared in this picture. Changes in displacements at crest level of dam in river direction have been shown by Fig. 7. In Fig. 7, the horizontal axis indicated the distance of nodes from central cantilever. Variations of arch stresses along crest of the dam can be checked over in Fig. 8. The same variation for cantilever stresses can be found in Fig. 9.

Regard to curves presented in Fig. 5, it can be deduced that the movements of dam body along the central cantilever in upstream-downstream direction have been increased when contraction joints are considered in modeling in compare to situation which effect of these joints has been neglected in simulation process. The extent of this increase is about approximately 100% for two mode of loading (thermo-static and only static loads). Another important result which can be concluded from this figure is that under the effect of thermal loads the body of the dam is moving back toward the upstream direction. This effect as it is obvious from the picture is significant. When

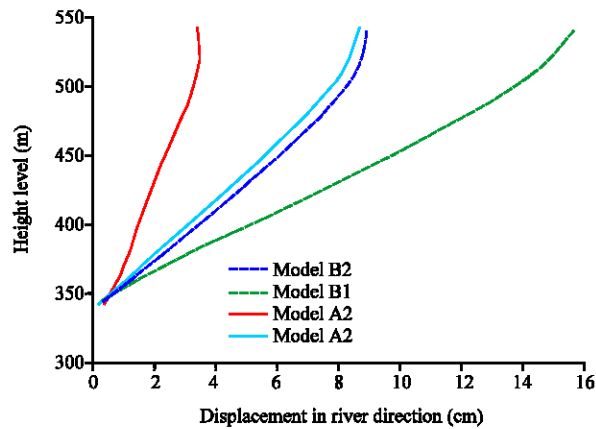


Fig. 5: Movements along the Karun-1 central cantilever in river direction

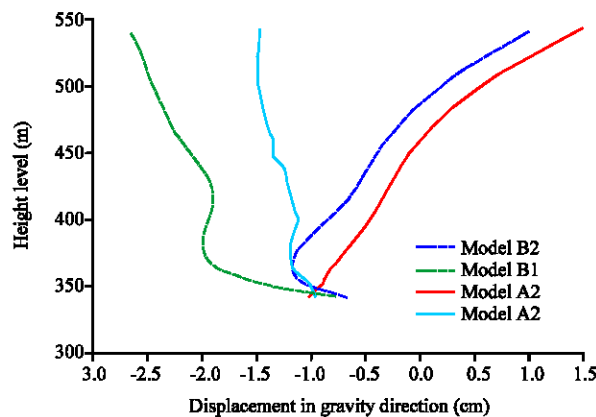


Fig. 6: Movements along the Karun-1 central cantilever in gravity direction

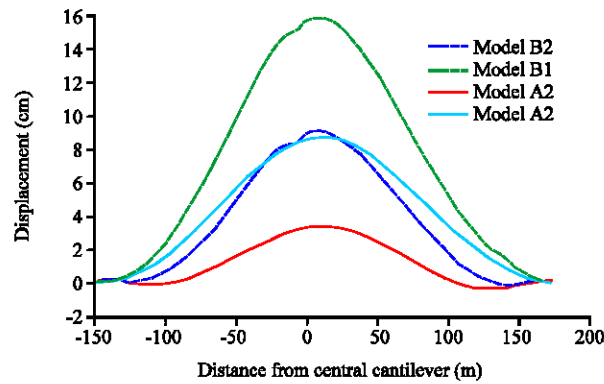


Fig. 7: Crest displacements in river direction

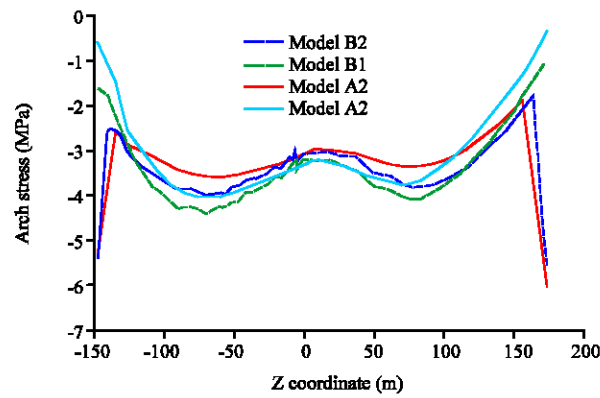


Fig. 8: Arch stresses variations along the dam crest

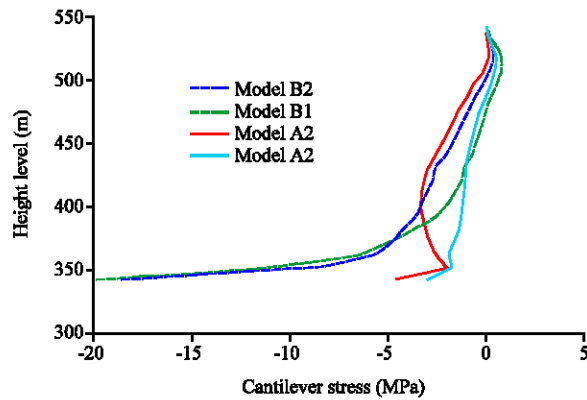


Fig. 9: Cantilever stresses alterations along central cantilever

thermal forces are included in analysis, the maximum displacement decreases approximately 50%. Furthermore, an interesting phenomenon which can be seen is that the effect of vertical contraction joints and thermal forces in Karun-1 arch dam is about the same, first in increasing and the second in decreasing the displacements in river direction (the curves belong to model A1 and B2 are very

close to each other). So, we can say that in the analysis of Karun-1 dam if any of two important factors e.g., contraction joints or thermal forces are not considered in data processing, the significant error in computing river direction displacements can be occurred. Another trivial result which can be observed from Fig. 5 is that from the base up to crest of the dam the displacements in river direction are increasing and maximum movements are happened in dam crest. When thermal loads are added to other existing static loads, e.g., gravity and hydrostatic loads, the central cantilever of the dam is moving upwards opposite to gravitational direction. This concept can be deduced from Fig. 6. In other words, this means that under the effect of heat transfer from downstream to upstream face of the dam in critical situation in summer season, the dam is turning toward the upstream direction about the basis. On the other hand, contraction joints cause the vertical displacements of dam become greater.

Figure 7 shows that displacements in river direction are symmetric about central cantilever axis of the dam. This is a logical result because Karun-1 dam has symmetrical plan and the loads applied to it including thermal forces are also symmetric to the mentioned axis. Vertical contraction joints have not meaningful effect on the values of arch stresses in Karun-1 dam. This can be shown through the examination of Fig. 8. This is a rational conclusion because the joints are orthogonal to the arch direction and under effect of thermo-static loads the arches would be compressed. So, these joints have not valuable effects on arch stresses. Another interesting result obtained from that picture could be the arch stress concentrations near the abutments in the models which consider the heat transfer e.g., model A2 and B2. This can be interpreted in this way: when heat transfer is applied to the dam, the non-homogeneity which exists between the dam and abutment in thermal conduction properties cause to the concentration of arch stresses in vicinity the dam-abutment line. This stress concentration also occurs for cantilever stresses due to the same reason (Fig. 9). As it can be seen from both Fig. 8 and 9, the arch and cantilever stresses along the crest and central cantilever respectively all have compressive nature. After surveying the principal stresses inside the dam (Table 1), it was obvious that under the effect of both contraction joints and thermal forces, the tensile stresses have been increased in dam body whereas near the abutments the mentioned stresses have been decreased. Not that the negative values in Table 1 present the compressive stresses whereas the positives reflect the tensile stresses. So, it is necessary that for

Table 1: Comparison between the maximum and minimum stresses

		Stress (Mpa)							
		Max. principle		Min. principle		Cantilever		Arch	
Type of analysis	Location	Max	Min	Max	Min	Max	Min	Max	Min
Model A1 and A2									
Without-temp analysis	Dam	5.00	-2.00	1.00	-5	3.00	-8.0	4.00	-9.00
With-temp analysis	Dam	4.00	-4.00	0.20	-15	2.00	-10.0	3.50	-10.00
Without-temp analysis	Near abutment	5.00	-6.00	2.30	-16	7.90	-14.0	4.00	-23.00
With-temp analysis	Near abutment	4.00	-13.00	0.20	-22	5.20	-17.0	3.50	-25.00
Model B1 and B2									
Without-temp analysis	Dam	1.00	-1.50	0.80	-13	1.00	-4.3	1.60	-5.23
With-temp analysis	Dam	0.20	-2.70	-0.26	-7	2.20	-6.5	1.00	-5.10
Without-temp analysis	Near abutment	8.50	-1.88	0.84	-24	4.70	-19.1	6.02	-7.50
With-temp analysis	Near abutment	8.33	-3.80	-0.30	-28	5.36	-20.4	3.53	-11.50

having more reliable assessment of tensile cracking potential in Karun-1 dam body, the heat transfer and contraction joints are being simultaneously considered in the stability analysis conjunction with hydrostatic and gravity loads. With respect to the results obtained in this study, the contribution of thermal loads in displacements and stresses is as the contribution of hydrostatic plus gravity loads. This result is in contrast to the conclusion which obtained by the Sheibani and Ghaemian (2006) for the Karaj arch dam.

CONCLUSION

The model which has been adopted via using ABAQUS package for Karun-1 dam has good potential for considering two important factor in stability evaluation of the mentioned dam; Contraction vertical joints and heat transfer in summer season. Because the resulted displacements from the model are coincidence with the values read from pendulum instruments located in central block of the dam. If one of these two factors is neglected in displacement or stress analysis, the significant errors would result in dam safety qualification.

REFERENCES

- Arabshahi, H. and V. Lotfi, 2009. Nonlinear dynamic analysis of arch dams with joint sliding mechanism. *J. Eng. Computat.*, 26: 464-482.
- Ardito, R., G. Maier and G. Massalongo, 2008. Diagnostic analysis of concrete dams based on seasonal hydrostatic loading. *J. Eng. Struct.*, 30: 3176-3185.
- Chen, X. and T. Hisada, 2007. Development of a finite element contact analysis algorithm to pass the patch test. *JMSE Int. J. Series A: Solid Mech. Mater. Eng.*, 49: 483-491.
- Christopher, B.J., 2007. *The Algebra of Geometry: Cartesian, Areal and Projective Co-ordinates.* Highperception Ltd., UK., ISBN: 978-1-906338-00-8.
- Du, X. and J. Tu, 2007. Nonlinear seismic response analysis of arch dam-foundation systems-part II opening and closing contact joints. *Bull. Earthquake Eng.*, 5: 121-133.
- Fenves, G.L., S. Mojtahedi and B.R. Reimer, 1992. Effect of contraction joints on earthquake response of arch dam. *J. Structural Eng.*, 118: 1039-1055.
- Franco, M. and G. Royer-Carfagni, 2005. Structured deformation of damaged continua with cohesive-frictional sliding rough fractures. *Eur. J. Mech. A Solids*, 24: 644-660.
- Jing, L. and J.Y. Chen, 2009. Seismic response analysis of arch dam with joints based on rate-dependant plastic damage model. *Proceedings of the 2009 International Conference on Engineering Computation*, May 02-03, Hong Kong, pp: 143-147.
- Li, N., M. Lou, J. Zhou and L. Xie, 2008. Seismic response of high-arch dams with contraction joints connected by springs and dampers. *China Civil Eng. J.*, 41: 94-99.
- Léger, P. and M. Leclerc, 2007. Hydrostatic, temperature, time-displacement model for concrete dams. *J. Eng. Mech.*, 133: 267-278.
- Léger, P. and S. Seydou, 2009. Seasonal thermal displacements of gravity dams located in Northern Regions. *J. Performance Constructed Facilitis*, 23: 166-174.
- Puso, M.A. and T.A. Laursen, 2002. A 3D contact smoothing method using Gregory patches. *Int. J. Numerical Meth. Eng.*, 54: 1161-1194.
- Sheibani, F. and M. Ghaemian, 2006. Effects of environmental action on thermal stress of Karaj concrete arch dam. *J. Eng. Mechanics*, 132: 532-544.

- Sheng, Z., Y. Xu and H. Liu, 2009. Research on seismic failure pattern of arch dam with contraction joints by shaking table tests and numerical analysis. *J. Hydroelectric Eng.*, 28: 69-74.
- Xinjia, L., X. Yanjie, W. Guanglun and Z. Chuhan, 2002. Seismic response of arch dams considering infinite radiation damping and joint opening effects. *J. Earthquake Eng. Eng. Vibration*, 1: 65-73.
- Zhang, C., Y. Xu, G. Wang and F. Jin, 2000. Non-linear seismic response of arch dams with contraction joint opening and joint reinforcements. *J. Earthquake Eng. Structural Dynamics*, 29: 1547-1566.
- Zhao, L., T. Li and Z. Niu, 2007. The dynamic contact model of nonlinear seismic response of high arch dams with contraction joints. *J. Hydroelectric Eng.*, 26: 91-95.